PROCEEDINGS, 44th Workshop on Geothermal Reservoir Engineering
Stanford University, Stanford, California, February 11-13, 2019
SGP-TR-214

Unravel Faults on Seismic Migration Images Using Structure-Oriented, Fault-Preserving and Nonlinear Anisotropic Diffusion Filtering

Kai Gao and Lianjie Huang

Los Alamos National Laboratory, Geophysics Group, Los Alamos, NM 87545

kaigao@lanl.gov; ljh@lanl.gov

Keywords: Fault, fracture, geothermal, structure-oriented filtering, fault-preserving filtering, nonlinear anisotropic diffusion filtering, Soda Lake

ABSTRACT

A high-resolution subsurface structural image can provide valuable information for optimizing well placement in geothermal exploration and production. A major challenge in imaging complex structures of geothermal fields is how to clearly reveal faults and fractures on seismic images. Land surface seismic data from geothermal fields are usually very noisy, resulting in noisy and low-resolution seismic migration images and, therefore, it is difficult to accurately detect faults/fractures on seismic images, particularly on 3D seismic migration images. We develop a structure-oriented, fault-preserving and nonlinear anisotropic diffusion filtering technique to greatly improve the quality of seismic migration images to facilitate fault interpretation. We employ a fast explicit diffusion scheme to significantly accelerate the computation of the nonlinear anisotropic diffusion, and employ computed coherence information from a seismic migration image itself to constrain the anisotropic diffusion process in space. The resulting parallel algorithm achieves structure-oriented, fault-preserving filtering accurately within minutes of computational time even for a large 3D seismic image volume. More importantly, the method simultaneously enhances continuous geological layers and discontinuous structures, such as faults and fracture zones, on seismic migration images. We apply our method to the 3D seismic migration image produced using 3D surface seismic data from the Soda Lake geothermal field, and obtain a greatly improved, high-resolution 3D seismic image volume that unravels several major and minor faults in this area, which are mostly invisible on the original seismic migration image. These faults are consistent with existing geological models and can be validated using the existing wells.

1. INTRODUCTION

Faults and fractures are channels for geothermal fluid flows. Fault locations, strikes, dips and orientations guide the optimal placement of geothermal well. Delineation of faults and fractures is therefore one of most important tasks for accurately characterizing reservoir properties of geothermal reservoirs. The Soda Lake geothermal field contains a particularly complex fault system as indicated in Fig. 1. There are numerous medium- to large-scale faults in this area with quasi-parallel orientations and steep dips.

Usually, the most straightforward approach for fault and fracture delineation is subsurface structural imaging with seismic imaging tools such as Kirchhoff migration, reverse-time migration (RTM), and least-squares reverse-time migration (LSRTM) when a higher-resolution image is needed. Most of these imaging tools can handle primary reflections well. However, faults/fracture zones in geothermal fields can have steep dips, posing significant challenges for these tools to efficiently and correctly reveal the locations and shapes of the faults. This is partially because structures with steep dips usually require long-offset seismic data to be imaged clearly, while land seismic data are usually short- to medium-offset. In addition, diffractions and noises of various kinds can severely deteriorate the signal-to-noise ratio of land seismic data, adding another layer of difficulty to accurate fault imaging. Although imaging methods such as wavefield-separation-based RTM (Fei et al., 2015) and LSRTM (Tan and Huang, 2014) can partially alleviate these problems, their capability in clearly delineating complex fault systems in geothermal fields is still inadequate.

We develop a computationally efficient structure-oriented, fault-preserving, 3D nonlinear anisotropic diffusion filter to delineate complex fault systems in 3D seismic migration images. Conventional numerical schemes (e.g., Fehmers and Höcker, 2003; Weickert, 1999) for solving the nonlinear anisotropic diffusion equation can be fairly slow for large 3D data volume because of the small step size required for a stable anisotropic diffusion time stepping process. To improve the computational efficiency, we employ a recently developed fast explicit diffusion (FED) scheme (Weickert, et al., 2016) to significantly accelerate the computation of the nonlinear anisotropic diffusion. The most important feature of this FED scheme is that it permits large time-step sizes in an explicit finite-difference framework. We also compute the coherence information from a seismic migration image to constrain the anisotropic diffusion process in space. We implement our filtering algorithm using a hybrid Message Passing Interface (MPI) and OpenMP parallel scheme.

The resulting parallel algorithm achieves structure-oriented, fault-preserving filtering accurately using only minutes of computational time even for a large 3D seismic image volume. Specifically, the method and numerical scheme can simultaneously enhance continuous geological layers and discontinuous structures, such as faults and fracture zones, on seismic migration images. We name our filtering algorithm the FED-based, structure-oriented, fault-preserving, nonlinear anisotropic diffusion filtering, or FED-SOFPAD for short. We apply our algorithm and code to the 3D seismic migration image volume produced using 3D land surface seismic data acquired at the Soda Lake geothermal field, and obtain a high-resolution 3D seismic image volume that unravels rich major and minor faults in this area. These faults are mostly invisible on the original seismic migration image. In addition, these delineated faults are consistent with existing geological models and can be validated using the existing geothermal injection/production wells.

2. METHODOLOGY

The structure-oriented, fault-preserving, nonlinear anisotropic diffusion filtering is described using the following diffusion-type partial differential equation (Fehmers and Höcker, 2003) with slight modification:

$$\frac{\partial u}{\partial t} = \nabla \cdot (\epsilon^m \mathbf{D} \nabla u), \tag{1}$$

where $u = u(\mathbf{x})$ is a noisy image, t is time, $\epsilon = \epsilon(\mathbf{x})$ is a spatially varying discontinuity scalar, $\mathbf{D} = \mathbf{D}(\mathbf{x})$ is an anisotropic diffusion tensor, and m is a positive power.

The computation of the anisotropic diffusion tensor is based on the so-called structural tensor defined by (Weickert, 1999)

$$\mathbf{S}(\mathbf{x}) = \nabla u (\nabla u)^{\mathrm{T}}, \tag{2}$$

where ∇u represents the spatial gradient of the image. The diffusion tensor $\mathbf{D}$ is then constructed based on the spectral decomposition of the spatially smoothed version of the structural tensor $\mathbf{S}(\mathbf{x})$ (e.g., Weickert, 1999).

The discontinuity scalar variable ϵ is crucial for fault perseverance during the anisotropic diffusion process. There are several different approaches to computing the discontinuities of an image. We adopt the following approach in the 3D case to compute the discontinuity:

$$\epsilon = 1 - \frac{2\sigma_2(\sigma_2 - \sigma_3)}{(\sigma_1 + \sigma_2)(\sigma_2 + \sigma_3)}, \tag{3}$$

where σ_1, σ_2 and σ_3 are the first, second and third eigenvalues of the structural tensor $\mathbf{S}(\mathbf{x})$ at spatial location $\mathbf{x}$, respectively. They are therefore spatially heterogeneous in most cases. The value of ϵ is small at faults and fractures, and large otherwise. One can also provide this discontinuity information using such as fault probability map (e.g., Wu and Fomel, 2018), which may lead to better filtering results.

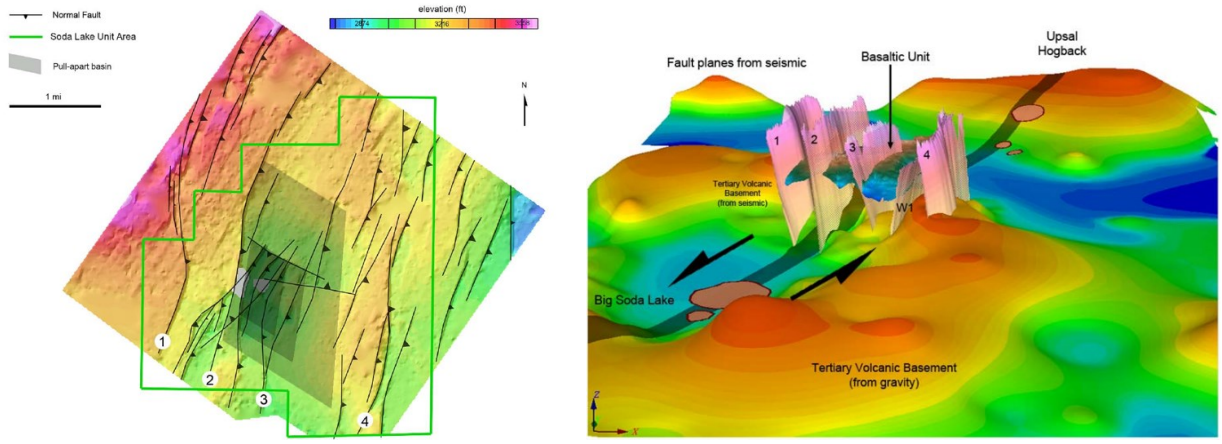

(a) (b)

Figure 1: Conceptual geological models for the Soda Lake geothermal filed. In the left panel (a), the black curves indicate the positions of the major faults in this area, while the right panel (b) shows several major faults and the basalt body in 3D (Magma Energy Corp., 2011)

The computational efficiency is a nontrivial problem for solving the nonlinear anisotropic diffusion equation (1). This is because it is necessary to use a sufficiently small time step size to achieve numerical stability when solving eq. (1). The computational time can be so long that for large 3D image volume even with high-performance computing (HPC) platforms.

We therefore adopt the FED finite-difference scheme (Weickert, et al., 2016) to conduct the temporal evolution. The most important feature of the FED scheme is that it allows much larger time step sizes compared with conventional explicit finite-difference schemes, leading to a computationally efficient algorithm to accurately solve eq. (1) even for large-scale 3D image volumes.

Specifically, the FED scheme for the nonlinear anisotropic diffusion can be represented as

$$u^{k+1,i+1} = (\mathbf{I} + \Delta t_i \mathbf{A}) u^{k+1,i}, \tag{4}$$

where k is the index of the outer update scheme, and i is the index of the inner update scheme, **A** is the system coefficient matrix resulting from the central finite-difference scheme associated with the spatial part of eq. (1), Δt_i is the time step size in the ith inner update scheme of the kth outer update scheme, and **I** is an identity matrix. The time step sizes vary during the temporal evolution, and satisfy

$$\Delta t_i \leq \frac{\Delta t_{\max}}{2\cos^2\left(\pi\frac{2i+1}{4n+2}\right)}, \tag{5}$$

where the maximum time step size is $\Delta t_{\max} = \frac{h^2}{2}$ with h being the grid size for the spatial finite-difference, and n is the total number of time steps in the inner update scheme.

The computational efficiency and accuracy of this FED scheme is superior to those of numerical schemes such as multigrid scheme or implicit scheme solved using the conjugate gradient method. This advantage is essential for applying our FED-SOFPAD filtering algorithm to large 3D image volumes with affordable computational costs.

3. NUMERICAL RESULTS

Subsurface structural imaging using RTM requires a depth-domain migration velocity model. We construct the depth-domain migration velocity model based on the time-domain migration velocity analysis result provided by Magma Energy (U.S.) Corp. Fig. 2 shows the depth-domain migration velocity model. The red-colored body in the center of the model is the high-velocity basaltic unit body shown in Fig. 1.

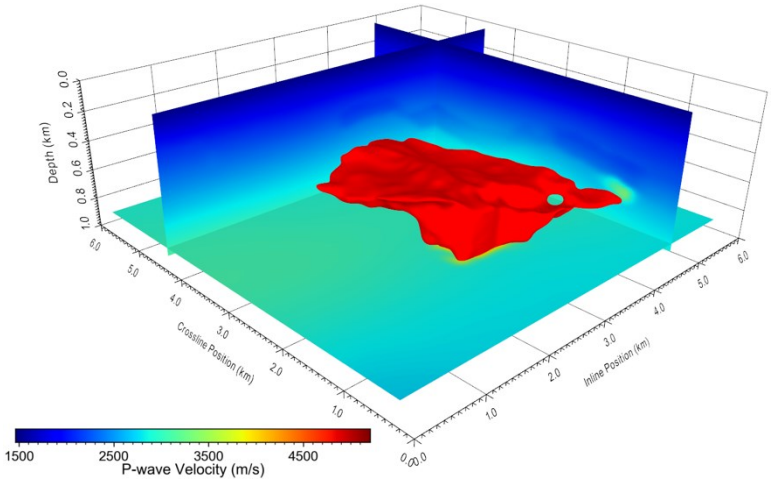

Figure 2: A slice view of the P-wave velocity model of the Soda Lake geothermal field. The red body in the center of the model represents the high-velocity basalt unit.

With this velocity model, we conduct reverse-time migration (Fei et al., 2015) using the processed common-shot gathers. To obtain high-resolution seismic image volume, we use a finer sampling in the depth direction (2.5 m) compared with the horizontal sampling (6.7 m). This ensures that the resulting structural image has high resolution in depth.

We obtain high-resolution subsurface structural images as shown in Fig. 3. Fig. 3(a) shows three inline slices and one crossline slice from the 3D image volume obtained with the wavefield-separation-based RTM. The resulting seismic image volume shows layered structures throughout the area. However, because there are noises and some insufficient data coverage, the seismic image volume is obviously contaminated with noises and migration artifacts. We apply our FED-SOFPAD filter to the 3D seismic RTM image volume, and obtain the filtered seismic image volume shown in Fig. 3(b). The continuity of most of the layers are evidently improved throughout the entire area. More importantly, faults are clearly revealed in the filtered seismic image volume. For instance, in the center inline slice at approximately 3.4 km of the crossline position, the faults are almost hidden beneath the artifacts and noises in the unfiltered seismic image volume. After the FED-SOFPAD filtering, at least seven faults are delineated on this slice above the basalt body, a significant improvement of imaging quality in this region. In addition, the image quality on the inline slices that are away from the basalt body are also improved, and the faults become clearer and sharper compared with the unfiltered image volume.

Fig. 4 shows another four slices of the image volume. Fig. 4(a) shows the unfiltered seismic image volume while Fig. 4(b) shows the FED-SOFPAD-filtered image volume. Similar to the comparison in Fig. 3, it is clear that after the FED-SOFPAD filtering, the faults' locations and shapes can be clearly delineated along both the inline and crossline directions, facilitating subsequent seismic interpretation.

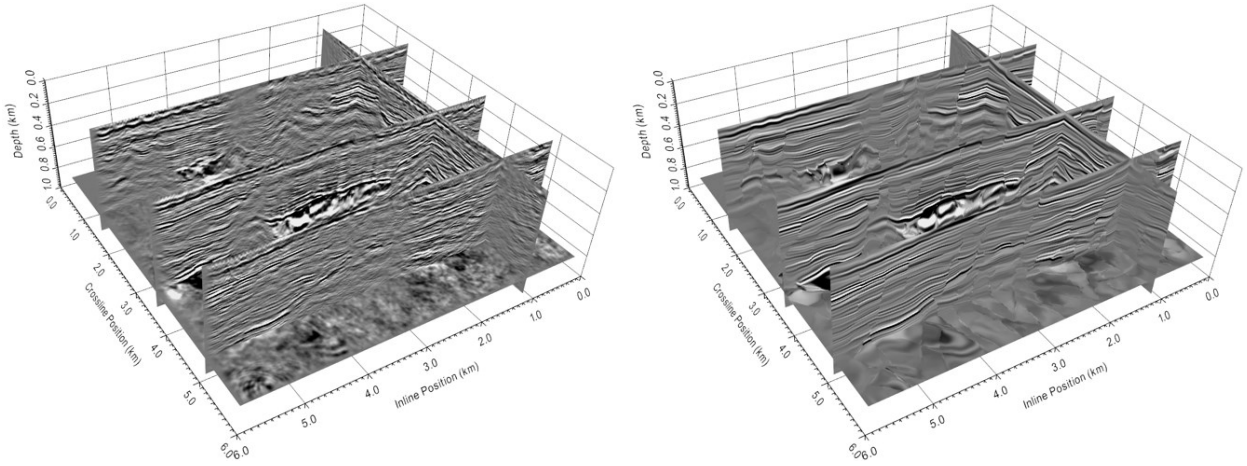

(a) Reverse-time migration image (b) FED-SOFPAD-filtered migration image

Figure 3: 3D subsurface structural image of Soda Lake geothermal field. The left panel (a) shows the unfiltered RTM structural image, while the right panel (b) shows the FED-SOFPAD-filtered structural image.

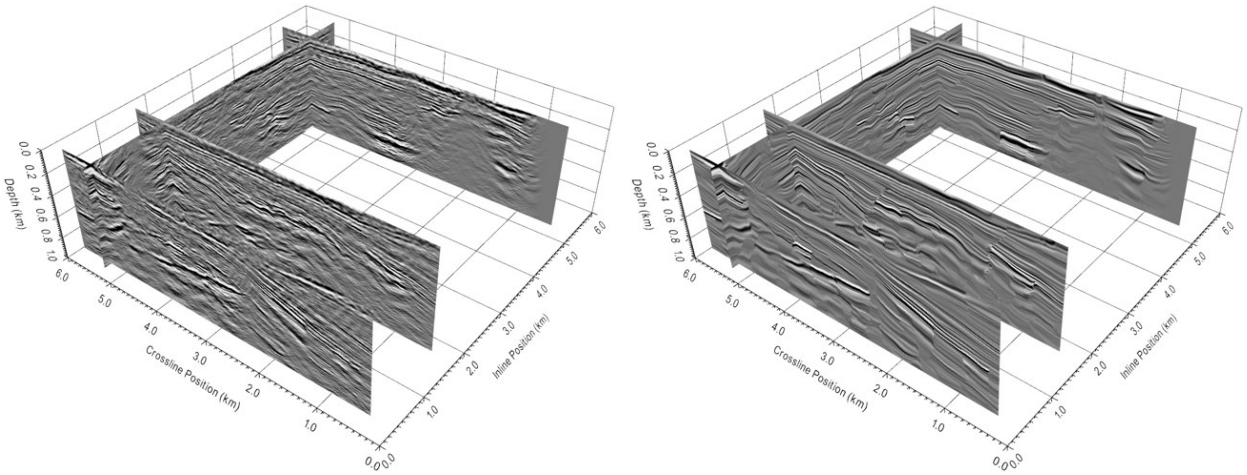

(a) Reverse-time migration image (b) FED-SOFPAD-filtered migration image

Figure 4: 3D subsurface structural image of Soda Lake geothermal field at a different view angle from that in Fig. 2 with different slices. The left panel (a) shows the unfiltered RTM structural image, while the right panel (b) shows the FED-SOFPAD-filtered structural image.

We show three plane-view images of the unfiltered and FED-SOFPAD-filtered seismic image volumes in Figs. 5, 6 and 7 for three different slice positions. Fig. 5(a) shows a crossline slice through the basalt body and an inline slice on the boundary of the basalt body. The depth of the horizontal slice is 0.4 km below the surface. Meanwhile, Fig. 5(b) shows the same three slices of the FED-SOFPAD-filtered image volume. There are several faults with steep dips in the FED-SOFPAD-filtered image that are obviously missing in the unfiltered image. Particularly, the FED-SOFPAD filtering reveals at least five major faults on top of the basalt body on the inline slice. The continuity of the geological layers shown in the crossline slice are greatly improved in the FED-SOFPAD-filtered image. The locations and orientations of these faults are more evidently revealed in the FED-SOFPAD-filtered image compared with the unfiltered image on the horizontal slices. The locations and orientations of the faults are generally consistent with those depicted in the conceptual geological model (Fig. 1).

Fig. 6 shows the comparison between the unfiltered and filtered seismic RTM images for another set of crossline and inline slices. The selected inline slice is away from the basalt body, while the crossline slice passes through the center of the basalt body. The improvement of image quality and the delineation of faults are significant on both the inline and crossline image slices. It is clear that the FED-SOFPAD filtering improves the continuity of layered structures while preserves the faults, or even improves the delineation of faults, for the Soda Lake geothermal field.

We show the last set of slices in Fig. 7. The comparison between the unfiltered and filtered seismic RTM image volume slices resembles the results in Figs. 5 and 6. For instance, we can find a fault-like structure at approximately 1.7 km along the inline direction of the unfiltered image (Fig. 7a). However, this fault-like structure is mostly deteriorated by noises and imaging artifacts in the unfiltered seismic image. This fault is clearly revealed on the inline slice of the FED-SOFPAD-filtered image (Fig. 7b). It is a fault with steep dip and produces obvious layer shifts in the depth direction. The improvement is also evident for several other large- or medium-scale faults on both the inline and crossline slices.

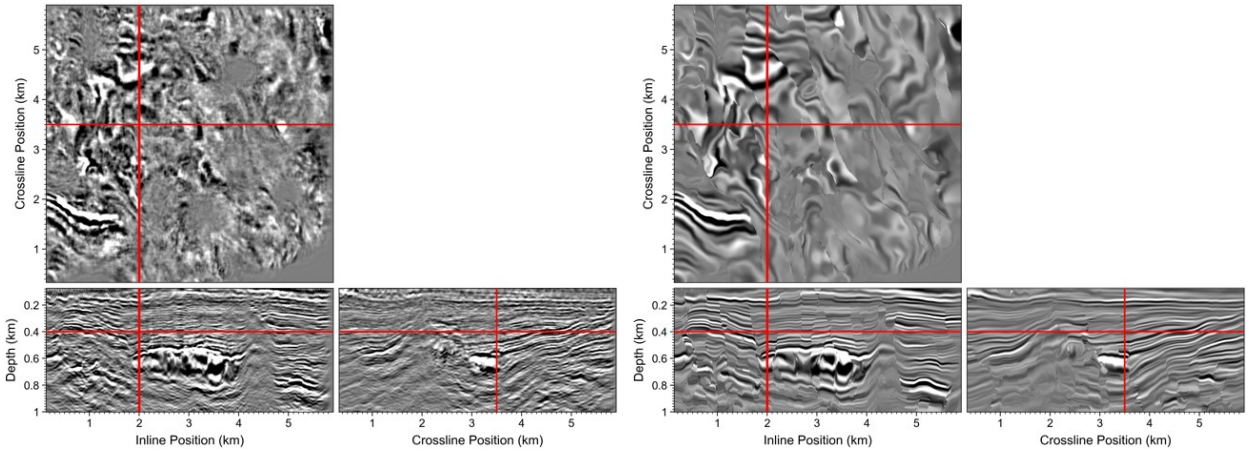

(a) Reverse-time migration image (b) FED-SOFPAD-filtered migration image

Figure 5: Plane view of the 3D subsurface structural image of Soda Lake geothermal field. The left panel (a) shows the RTM unfiltered structural image, while the right panel (b) shows the FED-SOFPAD-filtered structural image. Red lines indicate the slice positions.

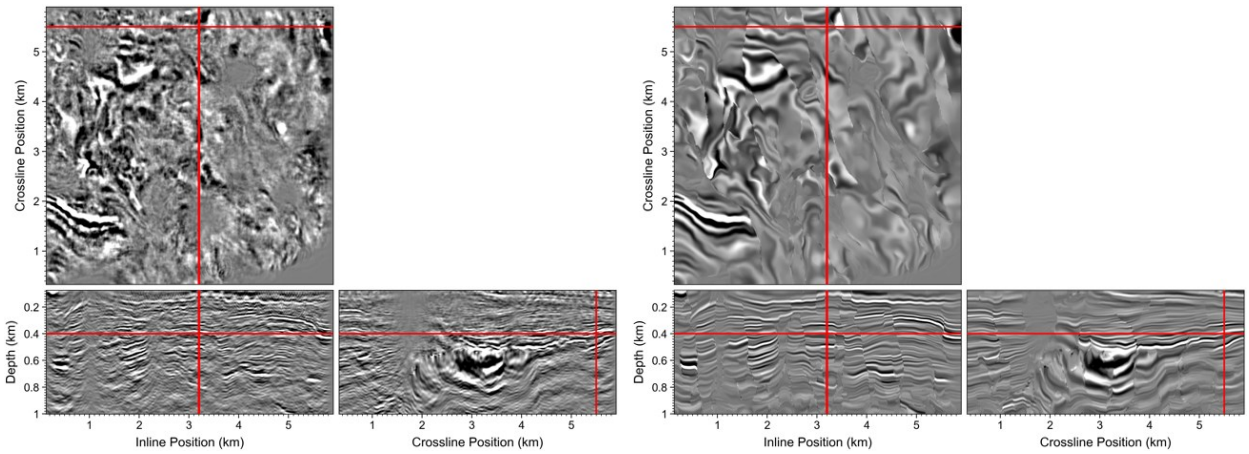

(a) Reverse-time migration image (b) FED-SOFPAD-filtered migration image

Figure 6: A second plane view of the 3D subsurface structural image of Soda Lake geothermal field. The left panel (a) shows the unfiltered RTM structural image, while the right panel (b) shows the FED-SOFPAD-filtered structural image. Red lines indicate the slice positions.

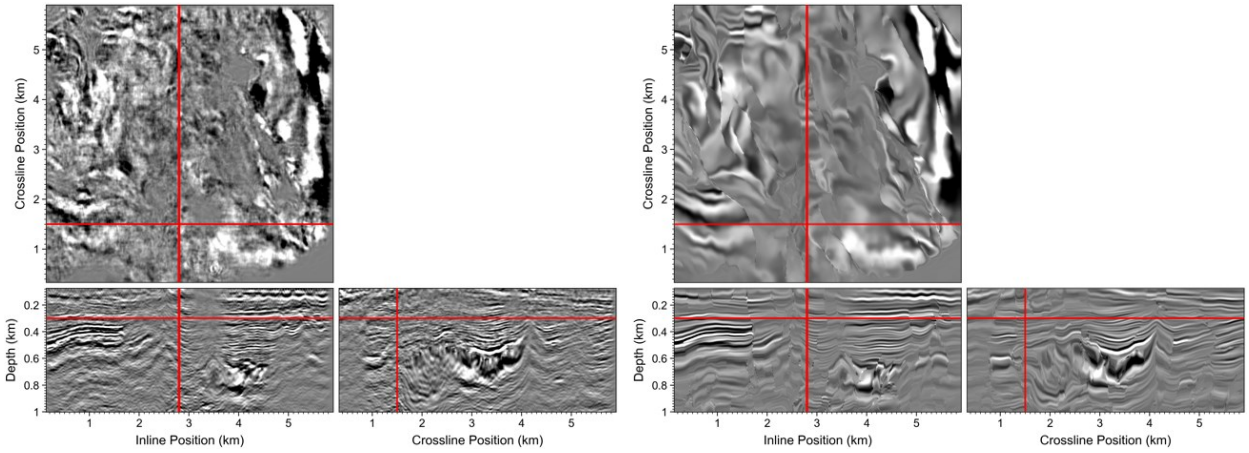

(a) Reverse-time migration image (b) FED-SOFPAD-filtered migration image

Figure 7: A third plane view of the 3D subsurface structural image of Soda Lake geothermal field. The left panel (a) shows the unfiltered RTM structural image, while the right panel (b) shows the FED-SOFPAD-filtered structural image. Red lines indicate the slice positions.

FED-SOFPAD filtering takes approximately 30 seconds for our MPI-OpenMP FED-SOFPAD code to conduct the filtering on 24 high-performance computing nodes. Each of these nodes contains 36 CPU cores. We use coarse-grain domain decomposition for the MPI parallelism and OpenMP thread parallelism within each node.

The results presented heretofore clearly show the capability of our FED-SOFPAD filtering algorithm and code to reduce noises and migration artifacts, improve the structural continuity, and delineate complex fault systems for large-scale 3D seismic image volumes.

CONCLUSIONS

We have developed a computationally efficient structure-oriented, fault-preserving, 3D nonlinear anisotropic diffusion filtering algorithm to unravel faults and fracture zones in seismic migration images. We implement the algorithm using a hybrid message passing interface and OpenMP parallel computing scheme. We have employed a fast explicit diffusion time evolution scheme to significantly improve the computational efficiency compared with conventional numerical schemes. We have applied our algorithm and code to the 3D seismic migration image volume obtained using 3D surface seismic data acquired at the Soda Lake geothermal field. The filtered image volume shows that our algorithm and code greatly improve the image quality with high computational efficiency. Subsurface layered structures become more continuous, while the faults that are almost invisible in the unfiltered image become sharply visible. The filtered image can serve as valuable guidance for geothermal well placement in the Soda Lake geothermal field. The results can also provide valuable geological information for structural interpretation for the Soda Lake geothermal field.

ACKNOWLEDGMENTS

This work was supported by U.S. Department of Energy through contract DE-AC52-06NA25396 to the Los Alamos National Laboratory (LANL). This research used resources provided by the Los Alamos National Laboratory Institutional Computing Program, which is supported by the U.S. Department of Energy National Nuclear Security Administration under Contract No. 89233218CNA000001. We thank Magma Energy (U.S.) Corp. for providing us with the field seismic data from the Soda Lake geothermal field.

REFERENCES

Fehmers, G.C. and Höcker, C.F.W., Fast structural interpretation with structure-oriented filtering, *Geophysics*, **68**(4), (2003), 1286-1293.

Fei, T.W., Luo, Y., Yang, J., Liu, H. and Qin, F., Removing false images in reverse time migration: The concept of de-primary, *Geophysics*, **80**(6), (2015), S237-S244.

Magma Energy (U.S.) Corp., 2011. Soda Lake DOE Phase I Report: Soda Lake 3D-3C Reflection Seismic Survey.

Tan, S. and Huang, L., Least-squares reverse-time migration with a wavefield-separation imaging condition and updated source wavefields, *Geophysics*, **79**(5), (2014), S195-S205.

Weickert, J., Grewenig, S., Schroers, C. and Bruhn, A., Cyclic schemes for PDE-based image analysis, *International Journal of Computer Vision*, **188**, (2016), 275-299.

Weickert, J., Coherence-enhancing diffusion of colour image, *Image and Vision Computing*, **17**, (1999), 201–212.

Wu, X. and Fomel, S., Automatic fault interpretation with optimal surface voting, *Geophysics*, **83**(5), (2018), O67-O82.